

Modeling to Evaluate a Spacecraft Propellant Gauging System

Jay Ambrose¹, Boris Yendler², and Steven H. Collicott³

INTRODUCTION

Prediction of remaining propellant is critical to the phasing of orbital replacements in the telecommunications industry. Increases in demand for data flow capacity have led to the development of larger and more powerful satellites. When such systems are utilized to full capacity, the net annual revenues per vehicle may be in the billions of dollars. Thus it is highly desirable to have very accurate predictions of the end of useful life for each vehicle to best manage the procurement and launch of orbital spares and replacements.

The liquid hydrazine propellant used for both orbit insertion and orbit station-keeping is stored in one or more large tanks with an internal passive capillary Propellant Management Device (PMD). The PMD controls liquid mass center and orients the liquid such that it can be extracted at the tank outlet. Typical PMDs are multiple thin vanes to orient the ullage bubble and a finer capillary structure near the tank outlet or sump. As the tank is emptied, a gas bubble grows in volume and is located away from the tank outlet by the PMD. The liquid collects in large fillet regions subtended by the vanes and tank walls. The liquid free surface forms a complex three-dimensional geometry not easily approximated by closed-form equations.

¹ Staff Engineer, Mechanical and Thermal Technology, Advanced Technology Center, Lockheed Martin, OL9-25/B205, 3251 Hanover St., Palo Alto, CA 94304-1191, Senior Member AIAA.

² Senior Staff System Engineer, Lockheed Martin Technical Operations, 1111 Lockheed Martin Way, Sunnyvale CA, 94089. Not an AIAA member.

³ Associate Professor, School of Aeronautics and Astronautics, 1282 Grissom Hall, Purdue University, West Lafayette, IN 47907-1282, Senior Member AIAA.

Various methods to determine remaining propellant quantity are in use, including bookkeeping, thermodynamic measurements, and capacitive sensors. Thermodynamic measurement methods such as the transient thermal response and gas law methods are attractive because of the simplicity of the required sensors. But such methods require an accurate assessment of the thermal response of the tank and propellant. Previous analyses have primarily been concerned with spherical tanks, and relatively simple thermal math models of the liquid and gas phases have been used with some success¹. However, an accurate representation of the three-dimensional liquid mass distribution, and hence, the free surface geometry in weightlessness is required to increase the measurement accuracy of such methods.

The goal is to determine the liquid free-surface geometry as a function of propellant fill level, transfer this geometry to a thermal finite-element model, and compute transient thermal response. Comparison of computed results to flight data and comparisons between computed results for slightly different liquid fill fractions show that the method can produce a viable propellant gauging system (PGS).

MODEL DESCRIPTION

Free Surface Model: The three-dimensional liquid and vapor distribution in the tank and PMD is solved for with Surface Evolver². Detailed three-dimensional analysis of fuel distribution in the vanes and sump of a propellant tank PMD has not been customary in spacecraft design and was not practical until the introduction of Surface Evolver³. See Ref. 4 for Surface Evolver convergence details and Ref. 5 for validation.

In a propellant tank with a vane-type PMD, there are three primary regimes of fill level, vane-dominated, transition, and fillet-dominated. At beginning of life large liquid quantities result in

the vane-dominated regime where a large bubble forms in the core. Depending upon extent of the bubble, it may shift in axial location or may be roughly centered by the primary vane edges. In this regime, there is generally a relatively thick layer of liquid separating the bubble from the tank wall. As the liquid level decreases, the bubble impinges on the wall and a transition to a fillet-dominated regime begins. At the lowest fill levels, the liquid is contained in fillets along the vane or vane-wall corners and the tighter capillary regions of the sump. The overall distribution of liquid is more tightly confined by the PMD in this fillet-dominated regime. With respect to the PGS measurements, the transition and fillet-dominated regimes are of primary interest, since it is later in life that accuracy of fuel measurements becomes crucial.

Liquid free surface geometries were predicted for the range of fuel loads in the tank and PMD geometry of the Lockheed-Martin A2100 class of GEO commercial communications satellites. A representative solution is shown in Fig. 1 for a vane-dominated case. The surface geometry is modeled in Surface Evolver by triangular facets that are then transferred to the solid modeling and meshing tool. It can be seen that the liquid forms a long nearly uniform fillet near the vane in the cylindrical region of the tank. Larger slugs of liquid form in the spherical dome regions of the tank, with the outflow dome containing approximately twice as much liquid as the opposite end.

Solid Model: The vertices of the facets of the interface solution were imported into the IDEAS solid modeling software, smoothed because of the finer resolution of the Surface Evolver model, and spline curves were generated through the points. A surface loft operation was used to generate the liquid free surface from the curves in I-DEAS⁶ Master Modeler. The liquid surface was stitched together with surfaces representing the tank wall, vane, and $\pi/4$ symmetry plane to

create a 1/4-tank liquid volume. For each case, curves corresponding to 5 circumferential angles within the 1/4-tank model were used, although more curves were available.

Finite Element Model: The solid model geometry was first partitioned at the tank equator in addition to other planes to allow more accurate meshing. For the fillet-dominated regime cases, one half of the one-eighth slice was meshed, corresponding to the liquid outflow end of the tank, which contains more liquid than the opposite end. The 1/8-tank mesh was reflected to create a one-quarter circumferential section of half the tank. The one-quarter slice was meshed to allow examination of various heater configurations. A summary of the four finite element models used in this study to assess PGS resolution and the solid models used to produce them are given in Table 1.

Thermal Model: The FEM produced to represent the liquid geometry was then used to create the thermal model. First, the geometry was partitioned into regions to aid in the meshing process. Then the liquid region was meshed in I-DEAS Simulation Module⁶ with solid linear tetrahedral elements. Additional triangular shell elements were added to represent the wall. These elements include the approximate thickness and the effect of the composite overwrap in the cylindrical region. Shell elements were also added to the liquid free surface in the area adjacent to the dry wall region. These were used to simulate the gas conduction between the dry wall region and the adjacent liquid layer. Material and physical properties used in the model are listed in Table 2.

In addition to the assumptions inherent in the translation of the chosen geometry into a FEM mesh, key assumptions were made with respect to heat transfer. In particular, the liquid and gas are both modeled as solids, assuming negligible convection effects. This assumption may be violated if large temperature gradients at the free surface cause substantial thermal-capillary

convection or if the gravity gradient induces thermal convection. As convective heat transfer is not modeled, the model will be in error if non-negligible convection exists. Another key assumption is that the helium gas is assumed to be a secondary path for heat transfer, and is modeled as a single non-geometric element. This element is coupled to the dry wall shell elements and the adjacent hydrazine surface elements with an area-proportional conductor. The heat transfer coefficient was based on assuming approximately half of the gas volume was effective, resulting in an estimated value of $2 \text{ W/m}^2\text{-K}$. This simplification was necessitated by the need to maintain sufficiently large element capacitance-resistance factors for computational accuracy and speed. Validity of this assumption was assessed by comparison with a two-dimensional thermal-network model (SINDA) that includes gas-phase conduction, and found to be in fair agreement. The inaccuracy introduced has little effect in the dome region, where the large mass and conductance of the liquid dominates.

The radiation heat loss from the tank was modeled using a non-geometric sink element that encloses the entire tank volume. The radiative coupling was based on an effective emittance of 0.016, which was determined from thermal balance measurements for a representative tank. The surroundings were held at a fixed temperature.

The heater boundary condition was modeled by applying heat sources directly to the wall shell elements. This simplification is deemed appropriate due to the thinness of the heater and tank wall. Various generic heater geometries were modeled including a uniform heat input to the dome region as well as discrete strip heaters typical of a flight design. Two analysis cases and corresponding boundary conditions are modeled in the current work. One is with the strip heaters and a relatively large liquid fill representative of a beginning of life case. This analysis case was compared with flight thermal data for a beginning of life case. Fill estimates for this

case are based on the bookkeeping method. Prediction of propellant fill using the bookkeeping method is more accurate closer to the beginning of life, thus producing a known case for comparison. The second analysis case is the arbitrary case with a middle of life propellant fill and uniform heater geometry. The purpose of this case is to estimate the measurement uncertainty for a particular heat input profile and fill level.

RESULTS

Predictions were first made for the specific case of beginning of life fill quantity to support validation of the thermal model. These results are compared to the flight data in Fig. 2. The sink temperature was held at 18.4 °C throughout the 90-hour transient. No flight data were available for the sink environment, but it is likely that it varied over the period of nearly four orbits. Agreement between the predicted and measured temperatures at cylinder sensor locations deviates by about 3 °C near the end of the transient. Near beginning of life, the propellant geometry is in the vane-dominated regime as discussed earlier. Therefore, this comparison is not a rigorous validation of the model for the middle or end of life cases but is used mainly as a qualitative validation of the modeling approach.

Transient runs for measurement uncertainty cases were initiated for each fill level with a uniform initial temperature of 20 °C and a 20 °C sink temperature. The heating boundary condition used was 100 W total heat load distributed evenly over the dome region of the tank wall. Representative temperature distributions for the tank wall are shown in Fig. 3 after 10 hours of heat input with a uniform initial temperature. One-quarter of the tank circumference and one-half of the length is shown. The hot spot corresponds to the location of the thinnest liquid layer where the gas bubble is beginning to extend into the dome region of the tank. This location is thus a good location for the sensor to maximize resolution of different liquid fill

quantities. The selected sensor location is at an angle bisecting two of the four major vanes and at the boundary between the dome and cylinder portions of the tank wall.

Predictions were generated for the four fill levels with the same heat input profile, boundary and initial conditions. Predicted temperatures at the selected sensor location (dome/cylinder boundary) are given in Fig. 4 for each of the four fill levels for the case of 100 W heating on the dome (25 W on the FEM). The key to resolving different fill levels is the ability to obtain temperature measurements that are sufficiently different to ensure accuracy. The minimum discernable difference in temperature sensor readings was taken to be approximately 1.0 °C based on the on-board analog to digital conversion method. It can be seen that after an hour of heating, the predicted temperatures at the sensor location for the different fill levels have sufficient spread to be easily distinguished.

The temperature rise after 10 hours of heat input is plotted versus fill quantity in Fig. 5. From these results it is estimated that the minimum fill quantity difference which can be resolved is approximately 3% at the nominal fill quantity of 245 kg. The trend is toward greater accuracy at smaller fill quantities.

CONCLUSIONS

Prior analytical correlations to the transient thermal response method have used relatively crude assumptions with respect to the liquid mass distribution in weightlessness. These assumptions have limited the ability to determine the measurement resolution of the method. By utilizing state-of-the-art modeling of the liquid-vapor interface a more accurate thermal math model of the propellant liquid free surface has been developed. The model was shown to be in fair agreement with flight data for beginning-of-life fill quantities from bookkeeping.

Further predictions were performed to estimate the attainable accuracy of the method for middle of life fill levels. The accuracy of the method is constrained by several factors. The dominant factor is the resolution of the temperature measurement system. The accuracy of the measurement is therefore tied to the minimal discernible difference in transient temperature rise between two liquid fill quantities. Since the temperature measurement resolution is known, predictions were made for various liquid fill increments to determine what the required change in fill quantity is for the given measurement resolution. These analyses yield an estimate of the gauging system accuracy.

REFERENCES

1. Purohit, G .P., Vu, C. C., and Dhir, V. K., "Transient Lumped Capacity Thermodynamic Model of Satellite Propellant Tanks in Micro-Gravity," AIAA Paper 99-1088, Jan. 1999.
2. Brakke, K. A. "The Surface Evolver," *Experimental Mathematics*, Vol. 1, No. 2, 1992, pp. 141-165.
3. Tegart, J., "A Vane-Type Propellant Management Device", AIAA Paper 97-3028, July 1997.
4. Collicott, S. H., "Convergence Behavior of Surface Evolver Applied to a Generic Propellant Management Device," AIAA Paper 99-0846, Jan. 1999.
5. Collicott, S. H., Bayt, R. L., and Courtney, S. D., "Ullage Bubble Stability in the Gravity Probe-B Helium Tank," AIAA Paper 94-3026, Jun. 1994.
6. "I-DEAS Design User's Guide", Structural Dynamics Research Corporation, Milford Ohio, 1999.

Table 1. Finite Element Model Summary

Calculated Mass, kg	# Solid Elements	# Shell Elements	Total Model Capacitance, J/K
227.0	9046	1778	1.222×10^5
232.3	7198	2083	1.292×10^5
243.8	6938	2170	1.304×10^5
277.7	5358	1206	1.489×10^5

Table 2. Model Material and Physical Property Summary. Cylinder wall values are based on titanium with graphite-epoxy over-wrap.

Location	Density kg/m ³	Conductivity W/m-K	Specific Heat J/kg-K	Wall Thickness mm
Cylinder Wall	3257	7.3	935	1.98
Dome Wall	4506	16.4	527	1.75
Hydrazine	1003	0.49	3084	NA

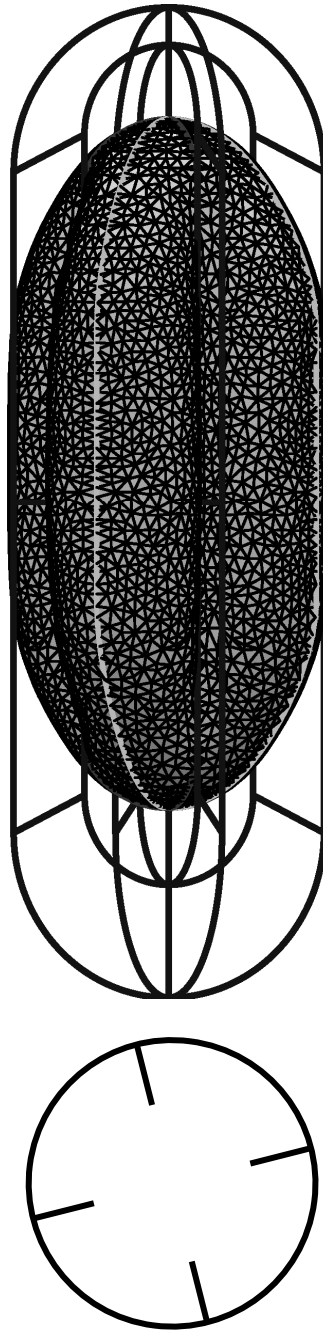


Fig. 1. Free surface geometry predicted with *Surface Evolver*: vane-dominated regime with tank and vane cross section at tank center shown.

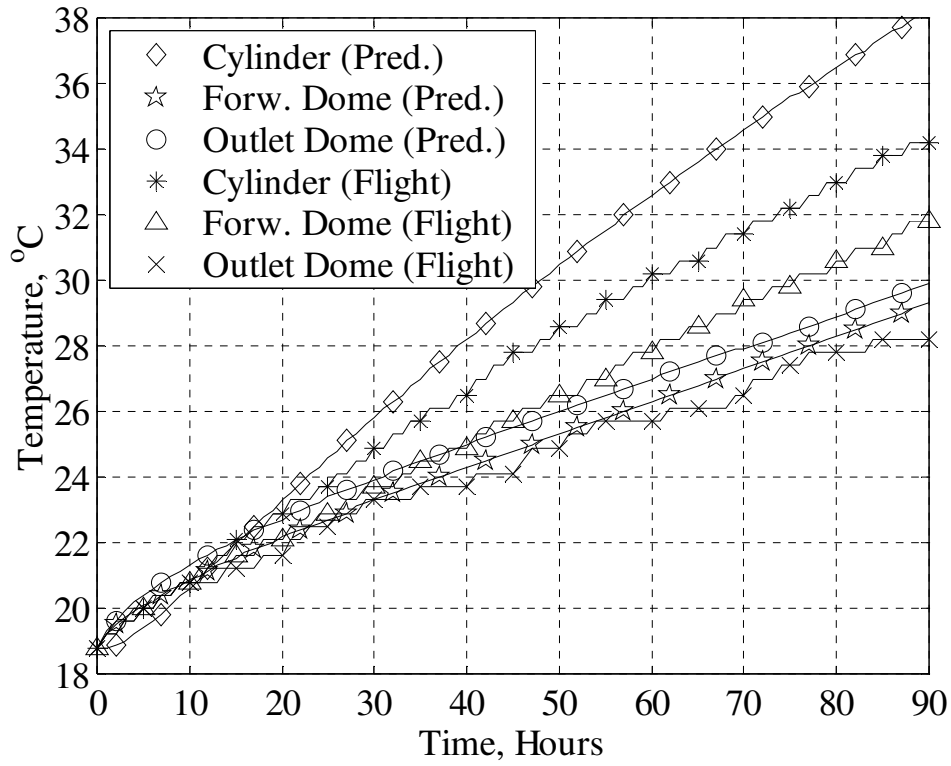


Fig. 2. Representative results – predicted versus flight test.

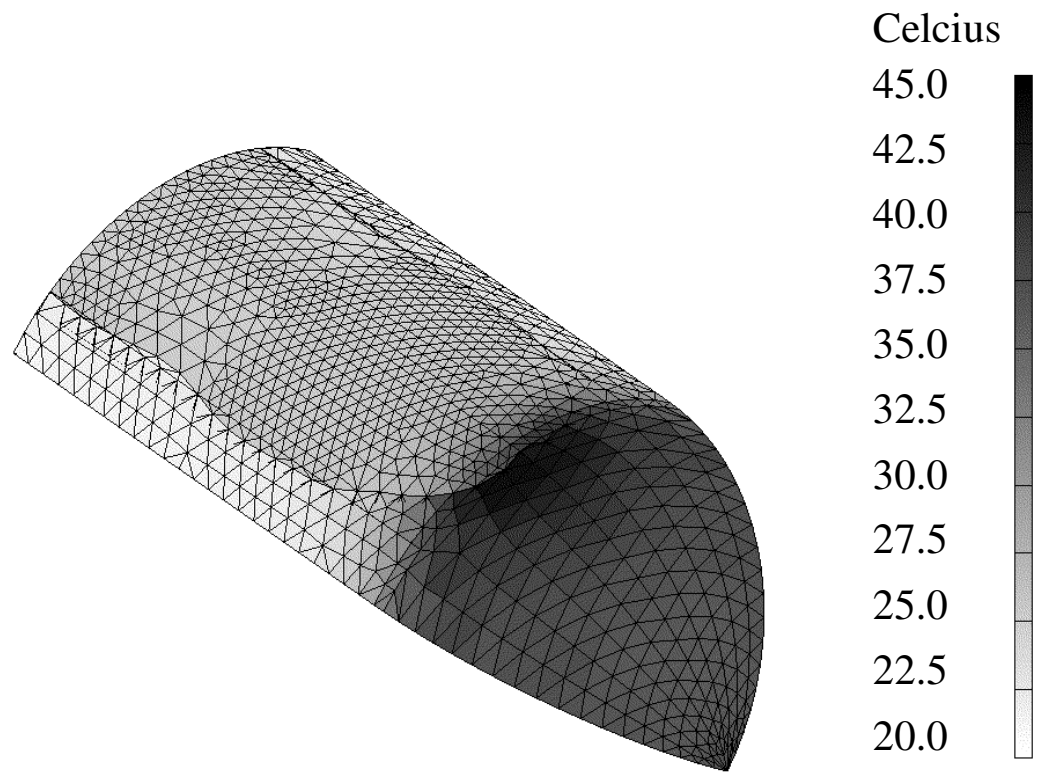


Fig. 3. Wall temperature profile after a 10-hour heating period.

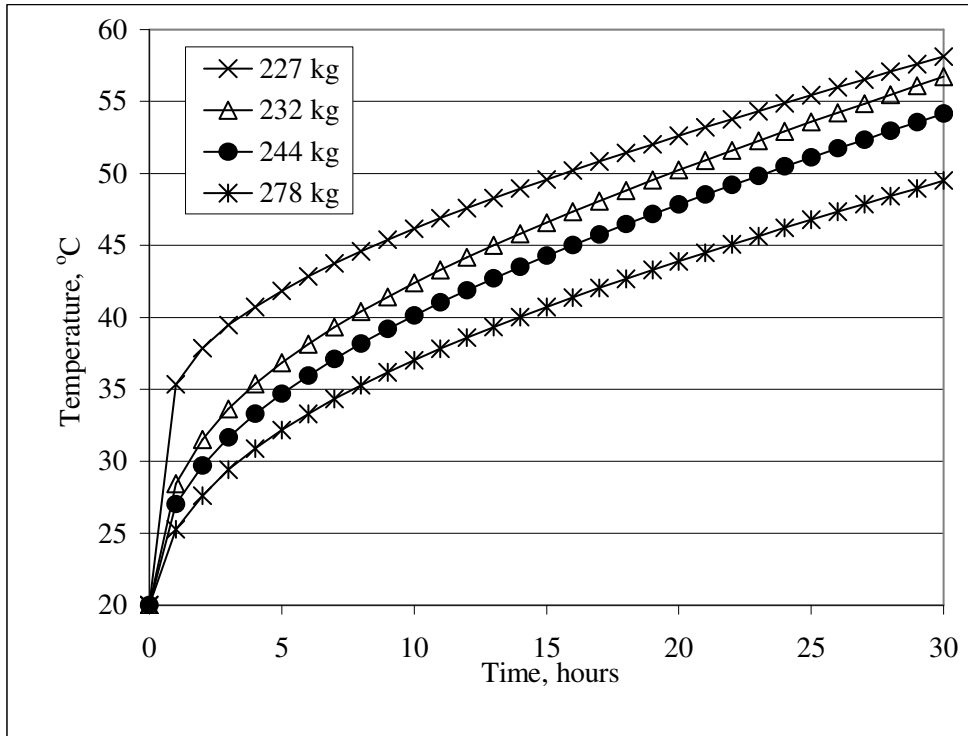


Fig. 4. Predicted transient wall temperature response versus fill level.

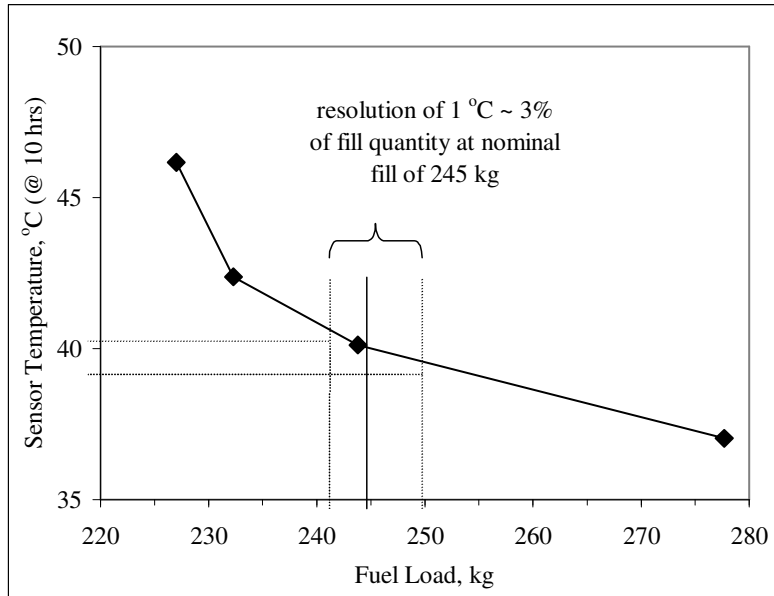


Fig. 5. Maximum wall temperature versus fill level.

List of Figure Captions

Fig. 1. Free surface geometry predicted with *Surface Evolver*: vane-dominated regime with tank and vane cross section at tank center shown.

Fig. 2. Representative results – predicted versus flight test.

Fig. 3. Wall temperature profile after a 10-hour heating period.

Fig. 4. Predicted transient wall temperature response versus fill level.

Fig. 5. Maximum wall temperature versus fill level.